Inorg. Chem. **2009**, *48*, 902−914

Geometric Isomerism in Pentacoordinate Cu^{2+} Complexes: Equilibrium, Kinetic, and Density Functional Theory Studies Reveal the Existence of Equilibrium between Square Pyramidal and Trigonal Bipyramidal Forms for a Tren-Derived Ligand

Andrés G. Algarra,[†] Manuel G. Basallote,*[,†] Carmen E. Castillo,[†] M. Paz Clares,[‡] Armando Ferrer,[†] Enrique García-España,*[,‡] José M. Llinares,[§] M. Angeles Máñez,[†] and Conxa Soriano[§]

Departamento de Ciencia de Materiales e Ingeniería Metalúrgica, Facultad de Ciencias, Universidad de Cádiz, Apartado 40, Puerto Real, 11510 Cádiz, Spain, Instituto de Ciencia Molecular (ICMOL), Departament de Química Inorgànica, Facultat de Química, Universitat de València, Paterna, Spain, and Instituto de Ciencia Molecular (ICMOL), Departament de Química Orgànica, Facultat de Farmàcia, Universitat de València, Burjassot, Spain

Received July 11, 2008

A ligand (**L1**) (bis(aminoethyl)[2-(4-quinolylmethyl)aminoethyl]amine) containing a 4-quinolylmethyl group attached to one of the terminal amino groups of tris(2-aminoethyl)amine (tren) has been prepared, and its protonation constants and stability constants for the formation of Cu^{2+} complexes have been determined. Kinetic studies on the formation of Cu^{2+} complexes in slightly acidic solutions and on the acid-promoted complex decomposition strongly suggest that the Cu^{2+}−**L1** complex exists in solution as a mixture of two species, one of them showing a trigonal bipyramidal (tbp) coordination environment with an absorption maximum at 890 nm in the electronic spectrum, and the other one being square pyramidal (sp) with a maximum at 660 nm. In acidic solution only a species with tbp geometry is formed, whereas in neutral and basic solutions a mixture of species with tbp and sp geometries is formed. The results of density functional theory (DFT) calculations indicate that these results can be rationalized by invoking the existence of an equilibrium of hydrolysis of the Cu−N bond with the amino group supporting the quinoline ring so that Cu**L1**$^{2+}$ would be actually a mixture of tbp [Cu**L1**$(H_2O)]^{2+}$ and sp [Cu**L1**$(H_2O)_2]^{2+}$. As there are many Cu^{2+}−polyamine complexes with electronic spectra that show two overlapping bands at wavelengths close to those observed for the Cu^{2+}−**L1** complex, the existence of this kind of equilibrium between species with two different geometries can be quite common in the chemistry of these compounds. A correlation found between the position of the absorption maximum and the τ parameter measuring the distortion from the idealized tbp and sp geometries can be used to estimate the actual geometry in solution of this kind of complex.

Introduction

Cu^{2+} complexes with open-chain and macrocyclic polydentate amine ligands are frequently pentacoordinate,[1−9] although the complexes can adopt structures that can be described as either square pyramidal (sp) or trigonal bipyramidal (tbp) depending mainly on the actual nature of the ligand. The appearance of a coordination number of five is not limited to polyaza ligands, and there is even recent evidence that strongly suggests a pentacoordinate nature of the Cu^{2+} aqua ion.[10] Tripodal tetradentate ligands such as tris(2-aminoethyl)amine (tren, **L2**) (Chart 1) and tris(2-pyridylmethyl)amine (tpa) are known to favor tbp coordina-

* To whom correspondence should be addressed. E-mail: manuel.basallote@uca.es (M.G.B.), enrique.garcia-es@uv.es (E.G.-E.). Phone: +34 963864879 (E.G.-E.). Fax: +34 963864322 (E.G.-E.).
† Universidad de Cádiz.
‡ Departament de Química Inorgànica, Universitat de València.
§ Departament de Química Orgànica, Universitat de València.

(1) (a) Miyoshi, K.; Tanaka, H.; Kimura, E.; Tsuboyama, S.; Murata, S.; Shimizu, H.; Ishizu, K. *Inorg. Chim. Acta* **1983**, *78*, 23–30. (b) Meyer, M.; Fremond, L.; Espinosa, E.; Guilard, R.; Ou, Z. P.; Kadish, K. M. *Inorg. Chem.* **2004**, *43*, 5572–5587. (c) Duggan, D. M.; Jungst, R. G.; Mann, K. R.; Stuky, G. D.; Hendrickson, D. N. *J. Am. Chem. Soc.* **1974**, *96*, 3443–3450. (d) Nunes, R. M.; Delgado, R.; Cabral, M. F.; Costa, J.; Brandao, P.; Felix, V.; Goodfellow, B. J. *Dalton Trans.* **2007**, 4536–4545. (e) Divaira, M.; Mani, F. *J. Chem. Soc., Dalton Trans.* **1985**, 2327–2332.

10.1021/ic8013078 CCC: $40.75
Published on Web 12/29/2008

Chart 1

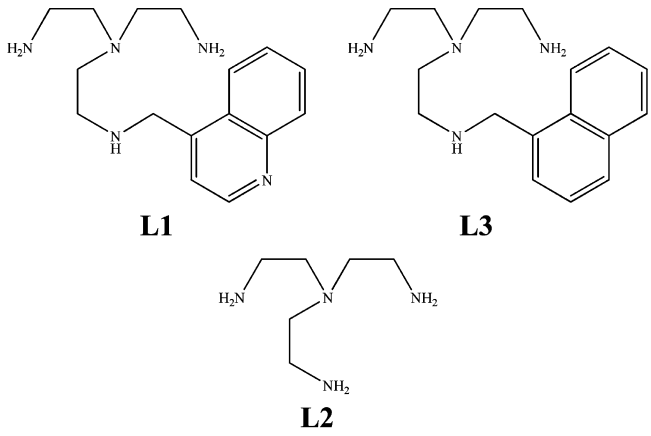

tion,[3−9] the remaining coordination site being occupied by water or any other ancillary ligand. In contrast, complexes with many other open-chain and macrocyclic polyamines display geometries close to sp coordination, the actual distortion depending on the ligand structure.[2,5]

Because of the diversity of structural distortions observed in pentacoordinate complexes efforts have been made to obtain quantitative measurements of such distortions, the most simple and useful being probably the τ parameter proposed by Addison et al.,[11] which is conceptually similar to the one previously proposed by Muetterties and Guggenberger.[12] The τ values are calculated according to eq 1, where α and β are the two largest L−M−L bond angles,[13] so that complexes with an ideal tbp structure have $\tau = 1$, those with ideal sp geometry have $\tau = 0$, and distorted complexes show τ values between 0 and 1.

$$\tau = (\alpha - \beta)/60 \quad (1)$$

The geometry that a given Cu^{2+}−polyamine complex adopts in solution can be reasonably deduced from the position of the absorption band in its electronic spectrum.[14] Pentacoordinate sp Cu^{2+} complexes usually show a band centered at ca. 580−670 nm,[15] whereas the maximum for tbp complexes appears at lower energy, typically at 780−950 nm.[6,7,16] Complexes showing an absorption band at intermediate positions can be assumed to have a geometry intermediate between both ideal polyhedra.[7,17] Although there are some examples of bi- and polynuclear complexes showing the coexistence of tbp and sp coordination,[18,19] most binuclear complexes show the same coordination environment for both metal centers.[9,14a,16a,20] However, there are many literature reports describing crystal structures of Cu^{2+} complexes adopting one of these geometries and showing an intense absorption band at the expected wavelength accompanied by weaker bands or shoulders at the wavelength corresponding to the other geometric arrangement.[6−8,18] In most cases those spectra are interpreted by considering that the appearance of the weaker band is inherent to the species whose structure is revealed in the X-ray analysis, a proposal supported by the observation of twin peaks of comparable intensity in the solid-state electronic spectra of some

(2) (a) Schatz, M.; Leibold, M.; Foxon, S. P.; Weitzer, M.; Heinemann, F. W.; Hampel, F.; Walter, O.; Schindler, S. *Dalton Trans.* **2003**, 1480–1487. (b) Alilou, E. H.; El Hallaoui, A.; El Ghadraoui, E.; Giorgi, M.; Pierrot, M.; Reglier, M. *Acta Crystallogr., Sect. C* **1997**, *53*, 559–562. (c) Su, C. Y.; Kang, B. S.; Wen, T. B.; Tong, Y. X.; Yang, X. P.; Zhang, C.; Liu, H. Q.; Sun, J. *Polyhedron* **1999**, *18*, 1577–1585. (d) Bencini, A.; Mani, F. *Inorg. Chim. Acta* **1984**, *87*, L9–L13. (e) Karlin, K. D.; Dahlstrom, P. L.; Hayes, J. C.; Simon, R. A.; Zubieta, J. *Cryst. Struct. Commun.* **1982**, *11*, 907–912. (f) Karlin, K. D.; Hayes, J. C.; Hutchinson, J. P.; Hyde, J. R.; Zubieta, J. *Inorg. Chim. Acta* **1982**, *64*, L219–L220.

(3) (a) Fabre, P. L.; Galibert, A. M.; Soula, B.; Dahan, F.; Castan, P. *J. Chem. Soc., Dalton Trans.* **2001**, 1529–1536. (b) Liu, Y. J.; Liu, Z. H. *Jiegou Huaxue* **1998**, *17*, 94. (c) Lu, Z. L.; Duan, C. Y.; Tian, Y. P.; You, X. Z. *Polyhedron* **1996**, *15*, 1769–1774. (d) Jacobson, R. R.; Tyeklar, Z.; Karlin, K. D.; Zubieta, J. *Inorg. Chem.* **1991**, *30*, 2035–2040. (e) Parker, R. J.; Spiccia, L.; Moubaraki, B.; Murray, K. S.; Skelton, B. W.; White, A. H. *Inorg. Chim. Acta* **2000**, *300*, 922–931. (f) Lim, B. S.; Holm, R. H. *Inorg. Chem.* **1998**, *37*, 4898–4908. (g) Corsi, D. M.; Murthy, N. N.; Young, V. G.; Karlin, K. D. *Inorg. Chem.* **1999**, *38*, 848–858. (h) Nagao, H.; Komeda, N.; Mukaida, M.; Suzuki, M.; Tanaka, K. *Inorg. Chem.* **1996**, *35*, 6809–6815. (i) Komeda, N.; Nagao, H.; Kushi, Y.; Adachi, G.; Suzuki, M.; Uehara, A.; Tanaka, K. *Bull. Chem. Soc. Jpn.* **1995**, *68*, 581–589. (j) Blackman, A. G. *Polyhedron* **2005**, *24*, 1–39.

(4) (a) Salam, M. A.; Aoki, K. *Inorg. Chim. Acta* **2001**, *314*, 71–82. (b) Jain, P. C.; Lingafelter, E. C. *J. Am. Chem. Soc.* **1967**, *89*, 6131. (c) Scott, M. J.; Lee, S. C.; Holm, R. H. *Inorg. Chem.* **1994**, *33*, 4651–4662.

(5) Karlin, K. D.; Hayes, J. C.; Juen, S.; Hutchinson, J. P.; Zubieta, J. *Inorg. Chem.* **1982**, *21*, 4106–4108.

(6) Marzotto, A.; Ciccarese, A.; Clemente, D. A.; Valle, G. *J. Chem. Soc., Dalton Trans.* **1995**, 1461–1468.

(7) Duggan, M.; Ray, N.; Hathaway, B.; Tomlinson, G.; Brint, P.; Pelin, K. *J. Chem. Soc., Dalton Trans.* **1980**, 1342–1348.

(8) Su, C. C.; Lu, W. S.; Hui, T. Y.; Chang, T. Y.; Wang, S. L.; Liao, F. L. *Polyhedron* **1993**, *12*, 2249–2259.

(9) Laskowski, E. J.; Duggan, D. M.; Hendrickson, D. N. *Inorg. Chem.* **1975**, *14*, 2449–2459.

(10) (a) Frank, P.; Benfatto, M.; Szilagyi, R. K.; D'Angelo, P.; Longa, S. D.; Hodgson, K. O. *Inorg. Chem.* **2005**, *44*, 1922–1933. (b) Pasquarello, A.; Petri, I.; Salmon, P. S.; Parisel, O.; Car, R.; Toth, E.; Powell, D. H.; Fischer, H. E.; Helm, L.; Merbach, A. E. *Science* **2001**, *291*, 856–859. (c) Yue, C. Y.; Lin, Z. Z.; Chen, L.; Jiang, F. L.; Hong, M. C. *J. Mol. Struct.* **2005**, *779*, 16–22.

(11) Addison, A. W.; Rao, T. N.; Reedijk, J.; Vanrijn, J.; Verschoor, G. C. *J. Chem. Soc., Dalton Trans.* **1984**, 1349–1356.

(12) Muetterties, E. L.; Guggenberger, L. J. *J. Am. Chem. Soc.* **1974**, *96*, 1748–1756.

(13) Alvarez, S.; Llunell, M. *J. Chem. Soc., Dalton Trans.* **2000**, 3288–3303.

(14) (a) Dittler-Klingemann, A. M.; Orvig, C.; Hahn, F. E.; Thaler, F.; Hubbard, C. D.; van Eldik, R.; Schindler, S.; Fabian, I. *Inorg. Chem.* **1996**, *35*, 7798–7803. (b) Dittler-Klingemann, A. M.; Hahn, F. E. *Inorg. Chem.* **1996**, *35*, 1996–1999. (c) Dittler-Klingemann, A. M.; Hahn, F. E.; Orvig, C.; Rettig, S. J. *Acta Crystallogr., Sect. C* **1996**, *52*, 1957–1959. (d) Basallote, M. G.; Duran, J.; Fernández-Trujillo, M. J.; Manez, M. A. *J. Chem. Soc., Dalton Trans.* **2002**, 2074–2079.

(15) (a) Georgousis, Z. D.; Christidis, P. C.; Hadjipavlou-Litina, D.; Bolos, C. A. *J. Mol. Struct.* **2007**, *837*, 30–37. (b) Gerard, C.; Mohamadou, A.; Marrot, J.; Brandes, S.; Tabard, A. *Helv. Chim. Acta* **2005**, *88*, 2397–2412. (c) Mautner, F. A.; Vicente, R.; Massoud, S. S. *Polyhedron* **2006**, *25*, 1673–1680. (d) Rosales, M. J.; Toscano, R. A.; Lunacanut, M. A.; Sosatorres, M. E. *Polyhedron* **1989**, *8*, 909–915. (e) Wang, Z. D.; Han, W.; Bian, F.; Liu, Z. Q.; Yan, S. P.; Liao, D. Z.; Jiang, Z. H.; Cheng, P. *J. Mol. Struct.* **2005**, *733*, 125–131.

(16) (a) Thaler, F.; Hubbard, C. D.; Heinemann, F. W.; van Eldik, R.; Schindler, S.; Fabian, I.; Dittler-Klingemann, A. M.; Hahn, F. E.; Orvig, C. *Inorg. Chem.* **1998**, *37*, 4022–4029. (b) Kuroda, R.; Mason, S. F.; Prosperi, T.; Savage, S.; Tranter, G. E. *J. Chem. Soc., Dalton Trans.* **1981**, 2565–2572. (c) Slade, R. C.; Tomlinson, A. A. G.; Hathaway, B. J.; Billing, D. E. *J. Chem. Soc. A* **1968**, 61. (d) Tyagi, S.; Hathaway, B. J. *J. Chem. Soc., Dalton Trans.* **1983**, 199–203.

(17) Ray, N. J.; Hulett, L.; Sheahan, R.; Hathaway, B. J. *J. Chem. Soc., Dalton Trans.* **1981**, 1463–1469.

(18) Massoud, S. S.; Mautner, F. A.; Abu-Youssef, M. A. M.; Shuaib, N. M. *Polyhedron* **1999**, *18*, 2061–2067.

(19) Shek, I. P. Y.; Lau, T. C.; Wong, W. T.; Zuo, J. L. *New J. Chem.* **1999**, *23*, 1049–1050.

(20) Duan, C. Y.; Lu, Z. L.; You, Y. Z.; Mak, T. C. W. *Transition Met. Chem.* **1998**, *23*, 77–79.

complexes whose crystal structure reveals the existence of a single geometric environment of the metal ion.[21] However, the alternative possibility of two bands in the electronic spectra caused by the existence of a mixture of geometric isomers in solution cannot be ruled out. In the present Article we present experimental and theoretical evidence illustrating the latter possibility for the case of a monosubstituted tren-based ligand. Ligand **L1** contains a 4-quinolylmethyl group attached at one of the terminal amino groups of tren, and it was initially prepared as a simple model to understand the behavior of a more complex macrocyclic ligand to be reported in the future. Nevertheless, during the course of kinetic work it became evident that Cu^{2+}−**L1** complexes exist in solution as a mixture of two different species, and density functional theory (DFT) calculations indicated that they do not arise from participation of the quinoline group in the coordination of the metal ion but from geometric isomerism accompanying hydrolysis of a Cu−N bond with one of the amino groups in the tren unit. The possibility of a similar process in unsubstituted tren (**L2**) is also explored.

Experimental Section

Synthesis of L1 (Bis(aminoethyl)[2-(4-quinolylmethyl)aminoethyl]amine). Quinoline-4-carbaldehyde (2.0 g, 12.7 mmol) dissolved in 300 mL of dry EtOH were added to *N*,*N*-bis(2-aminoethyl)ethane-1,2-diamine (5.6 g, 38.2 mmol) also dissolved in 300 mL of dry EtOH. The resulting solution was stirred for 2 h, and then $NaBH_4$ (2.2 g, 59 mmol) was added portionwise. After 2 h at room temperature, the solvent was evaporated to dryness. The resulting residue was treated with water and repeatedly extracted with dichloromethane (3 × 50 mL). The organic phase was then dried with anhydrous sodium sulfate, and the solvent was evaporated to yield the free amine as a yellowish oil. The oil was then taken in a minimum amount of EtOH and precipitated with aqueous HCl as its tetrahydrochloride salt (4.0 g, 73%). Mp: 210 °C (dec). ^{1}H NMR (D_2O): 2.94 (t, J = 6 Hz, 4H), 3.06 (t, J = 7 Hz, 2H), 3.18 (t, J = 6 Hz, 4H), 3.51 (t, J = 7 Hz, 2H), 5.10 (s, 2H), 8.01−8.08 (m, 2H), 8.17 (t, J = 7 Hz, 1H), 8.30 (d, J = 8 Hz, 1H), 8.39 (d, J = 8 Hz, 1H), 9.15 (d, J = 5 Hz, 1H). ^{13}C NMR (D_2O): 36.7, 45.6, 47.4, 48.8, 50.1, 121.8, 122.7, 124.4, 131.1, 135.3, 145.0. MS *m*/*z* (FAB): 288.0 $[M + H]^+$. Anal. Calcd for $C_{16}H_{29}N_5Cl_4 \cdot 1.5H_2O$: C, 41.77; H, 6.96; N, 15.2. Found: C, 42.0; H, 6.9; N, 15.1.

Electromotive Force Measurements. The potentiometric titrations were carried out at 298.1 ± 0.1 K using 0.15 M $NaClO_4$ or NaCl as supporting electrolyte. The experimental procedure (burette, potentiometer, cell, stirrer, microcomputer, etc.) has been fully described elsewhere.[22] The acquisition of the electromotive force (emf) data was performed with the computer program PASAT.[23] The reference electrode was a Ag/AgCl electrode in saturated KCl solution. The glass electrode was calibrated as a hydrogen-ion concentration probe by titration of previously standardized amounts of HCl with CO_2-free NaOH solutions, and the equivalent point was determined by the Gran's method,[24] which gives the standard potential, $E^{\circ\prime}$, and the ionic product of water (pK_w = 13.73(1)).

The computer program HYPERQUAD was used to calculate the protonation and stability constants.[25] The pH range investigated was 2.5−11.0, and the concentration of the metal ions and of the ligands ranged from 1×10^{-3} to 5×10^{-3} M with Cu^{2+}/**L1** molar ratios varying from 2:1 to 1:2. The different titration curves for each system (at least two) were treated either as a single set or as separated curves without significant variations in the values of the stability constants. Finally, the sets of data were merged together and treated simultaneously to give the final stability constants.

NMR Measurements. The ^{1}H and ^{13}C NMR spectra were recorded on a Bruker Advance 400 spectrometer operating at 399.96 MHz for ^{1}H and at 100.6 MHz for ^{13}C. For the ^{13}C NMR spectra, dioxane was used as a reference standard (δ = 67.4 ppm), and for the ^{1}H spectra, the solvent signal was used. Adjustments to the desired pH were made using drops of DCl or NaOD solutions. The pD was calculated from the measured pH values using the correlation, pH = pD − 0.4.[26]

Kinetic Experiments. The kinetics of decomposition of the Cu^{2+} complexes with the ligand **L1** was studied at 298.1 K using an Applied Photophysics SX17MV stopped-flow spectrophotometer provided with a PDA.1 diode array detector. The Cu^{2+}/**L1** ratio (1:1) and the pH of the starting solutions of the metal complexes were selected from the species distribution curves so that the concentration for one of the complex species is maximum while maintaining low concentrations of the other ones, using 0.15 M $NaClO_4$ as ionic strength. For this reason, only those species ($Cu\mathbf{L1}^{2+}$ and $Cu\mathbf{L1}(OH)^+$) which represent at least 80% of the total ligand under some conditions were studied. The solutions of the starting complexes were mixed in the stopped-flow instrument with solutions containing an excess of acid large enough to achieve pseudo-primer-order conditions. In all cases, the data for the acid-promoted decomposition of the complexes could be satisfactorily fitted using the SPECFIT program.[27] The kinetics of complex formation was measured at 298.1 K in the presence of 0.15 M $NaClO_4$ by mixing in the stopped-flow instrument solutions of Cu^{2+} and **L1** of the same concentrations and with the pH adjusted to the same value. The spectral changes were measured with the diode array detector and fitted to the desired kinetic model with program SPECFIT,[27] which provides the rate constant and the electronic spectra of the different species. As stated in the Results and Discussion section, the data were also refined with program Pro-KII.[28]

DFT Calculations. All DFT calculations were carried out with the Gaussian 03 software package[29] using the UB3LYP functional.[30,31] The Stuttgart−Dresden SDD basis set[32] was used with a relativistic effective core potential for Cu, and all ligand atoms (C, N, O, H) were described by the Pople-style basis set 6-31+G(d,p).[33] All geometry optimizations were performed without any symmetry constraints both in gas phase and in solvent, and efforts were made to find the lowest energy conformations by

(21) (a) Lever, A. B. P. *Inorganic Electronic Spectroscopy*, 2nd ed.; Elsevier: New York, 1984, pp 569−573. (b) Patel, R. N.; Singh, N.; Shukla, K. K.; Niclós-Gutiérrez, J.; Castiñeiras, A.; Vaidyanathan, V. G.; Unni Nair, B. *Spectrochim. Acta, Part A* **2005**, *62*, 261. (c) Tyagi, S.; Hathaway, B. J. *J. Chem. Soc., Dalton Trans.* **1981**, 2029–2033.

(22) García-España, E.; Ballester, M. J.; Lloret, F.; Moratal, J. M.; Faus, J.; Bianchi, A. *J. Chem. Soc., Dalton Trans.* **1988**, 101–104.

(23) Fontanelli, M.; Micheloni, M. In Program for the automatic control of the microburette and the acquisition of the electromotive force readings. *Proceedings of the I Spanish−Italian Congress on Thermodinamics of Metal Complexes*, Peñíscola, Castellón, Spain, 1990.

(24) (a) Gran, G. *Analyst* **1952**, *77*, 661–671. (b) Rossotti, F. J.; Rossotti, H. *J. Chem. Educ.* **1965**, *42*, 375–378.

(25) Gans, P.; Sabatini, A.; Vacca, A. *Talanta* **1996**, *43*, 1739–1753.

(26) Covington, A. K.; Paabo, M.; Robinson, R. A.; Bates, R. G. *Anal. Chem.* **1968**, *40*, 700–706.

(27) Binstead, R. A.; Jung, B.; Zuberbühler, A. D. *SPECFIT-32*; Spectrum Software Associates: Chappel Hill, NC, 2000.

(28) Maeder, M.; Neuhold, Y. M.; Puxty, G.; King, P. *Phys. Chem. Chem. Phys.* **2003**, *13*, 2836–2841.

Table 1. Stepwise Protonation Constants of **L1**, **L2**, and **L3** Determined at 298.1 ± 0.1 K in 0.15 M $NaClO_4$ or NaCl

reaction[a]	L1	L1[b]	L2[c]	L3[d]
$H + L \rightleftarrows HL$	9.74(1)[e]	10.36(2)	10.12	9.72(1)
$H + HL \rightleftarrows H_2L$	9.08(1)	9.37(1)	9.41	9.10(1)
$H + H_2L \rightleftarrows H_3L$	6.60(1)	7.10(1)	8.42	7.45(1)
$H + H_3L \rightleftarrows H_4L$	3.43(1)	3.72(1)		

[a] Charges omitted. [b] Values determined in 0.15 M NaCl. [c] Values determined in 0.1 M $NaClO_4$ taken from ref 2. [d] Values taken from ref 3, $I = 0.15$ M NaCl. [e] Values in parentheses are standard deviation in the last significant figure.

comparing the structures optimized from different starting geometries. Aqueous-phase calculations ($\varepsilon = 78.39$) were performed through the use of the conductor-like polarizable continuum model (CPCM)[34] as implemented in Gaussian 03.[29] In order to take into account the nonspecific water effect in the gas-phase geometry optimizations, the energy of the species obtained in the gas phase is given in the text as the result of single-point CPCM calculations.[34] Vibrational calculations were performed to confirm that the calculated structures were minima.

The electronic absorption spectra of the previously optimized species were calculated using the time-dependent DFT (TD-DFT) formalism,[35] and 30 or 40 singlet-excited-state energies were calculated for **L1** and **L2** complexes, respectively. The nonspecific solvent effect was considered in the TD-DFT calculations via the nonequilibrium version of the CPCM algorithm.[34]

Results and Discussion

Equilibrium Studies on Ligand Protonation and Formation of Cu^{2+} Complexes. Determination of the Protonation Constants of L1. The protonation constants of **L1** have been determined by pH-metric titrations at 298.1 ± 0.1 K in aqueous solution using either 0.15 M $NaClO_4$ or 0.15 M NaCl. The constants calculated using the HYPERQUAD set of programs[25] are collected in Table 1 together with those of the related polyamine tren (**L2**) taken from the literature[36] and those we have previously reported for the analogous ligand containing naphthalene at the place of quinoline (**L3**).[37] The corresponding species distribution diagram in 0.15 M $NaClO_4$ is shown in Figure 1.

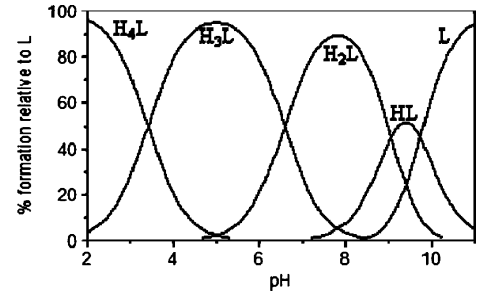

Figure 1. Distribution diagram for the protonated species of **L1** in 0.15 M $NaClO_4$.

L1 presents in the pH range of study four measurable protonation steps. The first two are relatively basic and separated between them by no more than one logarithmic unit. Third protonation brings about a further decrease in basicity; the separation between the second and third protonation being over two logarithmic units. Finally, the last protonation step is much less basic.

The downfield and upfield shifts in the ^1H and ^{13}C NMR spectra of protons and carbon nuclei placed at two-bond distance from the nitrogen atoms bearing protonation are very illustrative to establish average protonation sequences in polyamine compounds.[38] The ^1H NMR signals of the aromatic protons and particularly the doublet signal of proton **HQ3** placed at two-bond distance from the quinoline nitrogen bear an important downfield shift below pH 4.4 ($\Delta\delta = 0.4$ ppm) in correspondence with the protonation of this nitrogen (for the labeling see Figure 2A) In the same pH range the corresponding carbon atom **CQ3** shifts 6 ppm upfield (Figure 2B). Above this pH the observed changes are not significant. This would support that fourth protonation occurs at the nitrogen atom of the quinoline ring.

Also the analysis of the NMR spectra permits us to establish that the primary nitrogens are in average more basic and thereby protonate at a higher pH than the secondary amino group. Although protons labeled as **H1**, at two-bond distance from the primary nitrogens, experience their maximum downfield shift above pH 7.5 ($\Delta\delta = 0.4$ ppm), protons **H4** bear their maximum shift between pH 7.5 and 4.5 in correspondence with the third protonation of the free ligand. Confirming this sequence carbon atoms **C1** bear at upfield shift of ca. 6.00 ppm from pH 11 to 8, whereas **C3** in β-position with respect to the secondary nitrogen group experience its largest upfield ca. 3 ppm in correspondence with the third protonation of **L1** (Figure S1 in the Supporting Information).

(29) Frisch, M. J.; Trucks, G. W.; Schlegel, H. B.; Scuseria, G. E.; Robb, M. A.; Cheeseman, J. R.; Montgomery, J. A., Jr.; Vreven, T.; Kudin, K. N.; Burant, J. C.; Millam, J. M.; Iyengar, S. S.; Tomasi, J. J.; Barone, V.; Mennucci, B.; Cossi, M.; Scalmani, G.; Rega, N.; Petersson, G. A.; Nakatsuji, H.; Hada, M.; Ehara, M.; Toyota, K.; Fukuda, R.; Hasegawa, J.; Ishida, M.; Nakajima, T.; Honda, Y.; Kitao, O.; Nakai, H.; Klene, M.; Li, X.; Knox, J. E.; Hratchian, H. P.; Cross, J. B.; Adamo, C.; Jaramillo, J.; Gomperts, R.; Stratmann, R. E.; Yazyev, O.; Austin, A. J.; Cammi, R.; Pomelli, C.; Ochterski, J. W.; Ayala, P. Y.; Morokuma, K.; Voth, A.; Salvador, P.; Dannenberg, J. J.; Zakrzewski, V. G.; Dapprich, S.; Daniels, A. D.; Strain, M. C.; Farkas, O.; Malick, D. K.; Rabuck, A. D.; Raghavachari, K.; Foresman, J. B.; Ortiz, J. V.; Cui, Q.; Baboul, A. G.; Clifford, S.; Cioslowski, J.; Stefanov, B. B.; Liu, G.; Liashenko, A.; Piskorz, P.; Komaromi, I.; Martin, R. L.; Fox, D. J.; Keith, T.; Al-Laham, M. A.; Peng, C. Y.; Nanayakkara, A.; Challacombe, M.; Gill, P. M. W.; Johnson, B.; Chen, W.; Wong, M. W.; Gonzalez, C.; Pople, J. A. *Gaussian03*, revision B.04; Gaussian, Inc.: Pittsburgh, PA, 2003.
(30) Becke, A. D. *J. Chem. Phys.* **1993**, *98*, 5648–5652.
(31) Lee, C. T.; Yang, W. T.; Parr, R. G. *Phys. Rev. B* **1988**, *37*, 785–789.
(32) Hay, P. J.; Wadt, W. R. *J. Chem. Phys.* **1985**, *82*, 299–310.
(33) Schaefer, A.; Horn, H.; Ahlrichs, R. *J. Chem. Phys.* **1992**, *97*, 2571–2577.
(34) Cossi, M.; Rega, N.; Scalmani, G.; Barone, V. *J. Comput. Chem.* **2003**, *24*, 669–681.
(35) Casida, M. E.; Jamorski, C.; Casida, K. C.; Salahub, D. R. *J. Chem. Phys.* **1998**, *108*, 4439–4449.
(36) Motekaitis, R. J.; Martell, A. E.; Lehn, J. M.; Watanabe, E. I. *Inorg. Chem.* **1982**, *21*, 4253–4257.
(37) Clares, M. P.; Aguilar, J.; Aucejo, R.; Lodeiro, C.; Albelda, M. T.; Pina, F.; Lima, J. C.; Parola, A. J.; Pina, J.; de Melo, J. S.; Soriano, C.; Garcia-Espana, E. *Inorg. Chem.* **2004**, *43*, 6114–6122.
(38) (a) Bencini, A.; Bianchi, A.; Garcia-España, E.; Micheloni, M.; Ramirez, J. A. *Coord. Chem. Rev.* **1999**, *188*, 97–156. (b) Frassineti, C.; Alderighi, L.; Gans, P.; Sabatini, A.; Vacca, A.; Ghelli, S. *Anal. Bioanal. Chem.* **2003**, *376*, 1041–1052. (c) Frassineti, C.; Ghelli, S.; Gans, P.; Sabatini, A.; Moruzzi, M. S.; Vacca, A. *Anal. Biochem.* **1995**, *231*, 374–382. (d) Sarneski, J. E.; Surprenant, H. L.; Molen, F. K.; Reilley, C. N. *Anal. Chem.* **1975**, *47*, 2116–2124.

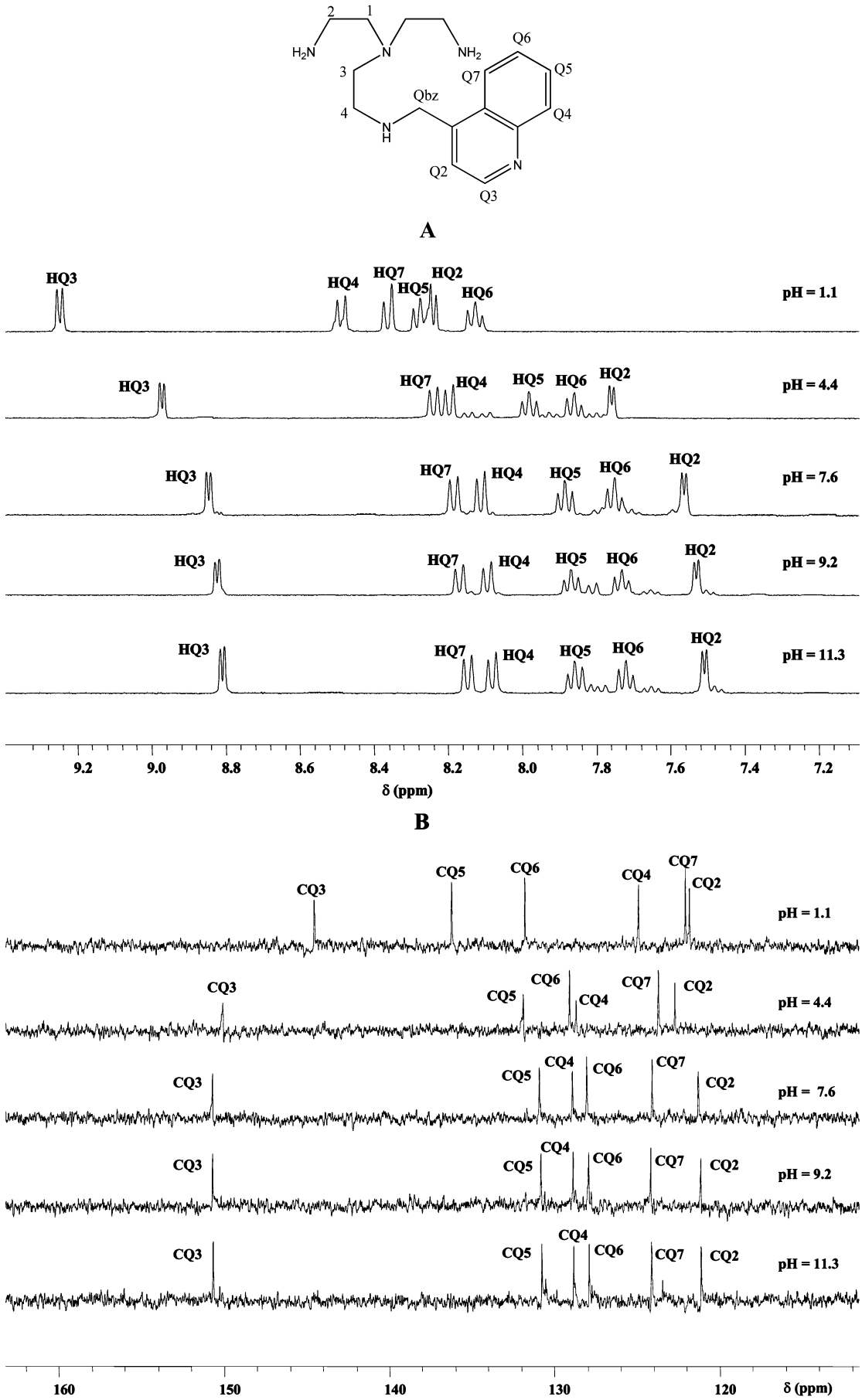

Figure 2. Variation with the pH of the aromatic region of the ^{1}H (A) and ^{13}C (B) NMR spectra.

Table 2. Logarithms of the Stability Constants for the Formation of Cu^{2+} Complexes by Ligand **L1** Determined at 298.1 ± 0.1 K in 0.15 M $NaClO_4$

reaction[a]	L1	L2[b]	L3[c]
$Cu + 2H + L \rightleftarrows CuH_2L$	24.98(2)[d]		
$Cu + H + L \rightleftarrows CuHL$	21.64(1)		21.25(2)
$Cu + L \rightleftarrows CuL$	16.93(1)	18.5	17.43(1)
$Cu + L + H_2O \rightleftarrows CuL(OH) + H$	7.96(1)		8.49(2)
$CuL + H \rightleftarrows CuHL$	4.71(1)		
$CuHL + H \rightleftarrows CuH_2L$	3.34(2)		3.82(2)
$CuL + H_2O \rightleftarrows CuL(OH) + H$	−8.97(2)	−9.2	−8.94(2)

[a] Charges omitted. [b] Values determined in 0.1 M $NaClO_4$ taken from ref 2. [c] Values taken from ref 3, $I = 0.15$ M NaCl. [d] Values in parentheses are standard deviation in the last significant figure.

Another point to be discussed is that, although the two first protonation constants of either **L1** or **L3**[37] are comparable to those of the parent polyamine tren, **L2**[36] their third protonation constant is clearly lower than that of tren, **L2**. This reduced basicity can be ascribed as confirmed by NMR to a third protonation process occurring predominantly at the secondary nitrogen atom. Finally, it has to be remarked that in the pH range studied we have not observed any protonation of the apical tertiary nitrogen. This can be ascribed to the lower basicity of tertiary amines in water due to their poorer solvation with respect to primary and secondary amines.[38]

Another interesting point concerns the higher values of the basicity constants obtained in NaCl with respect to $NaClO_4$, although these results can be interpreted in terms of interaction between the chloride ion and the protonated forms of the ligand (see the Supporting Information).

Determination of the Cu^{2+} Complexes Stability Constants. The Cu^{2+} stability constants determined by pH-metric titrations at 298.1 ± 0.1 K in aqueous solution are collected in Table 2. In order to avoid possible interferences from Cl^- anions we have just used $NaClO_4$ as ionic strength. Relevant data for the related ligands **L2** and **L3** taken from the literature[36,37] have also been included in the Table 2.

L1 forms with Cu^{2+} mononuclear species of $CuHq\mathbf{L1}^{(2+q)}$ stoichiometry with $q = -1, -2$. The value of the constant for the formation of the $Cu\mathbf{L1}^{2+}$ species is in line with those we have previously obtained for **L3**[37] and slightly lower than those reported for tren (**L2**).[36] These lower constants are related with the different types of donor groups that these tripodal polyamines have; whereas **L2** has only primary amino groups, **L1** and **L3** have two primary and one secondary amino which display different donor abilities and solvation characteristics in water. The additional protonation equilibrium present in the system Cu^{2+}−**L1** should imply the protonation of the nitrogen atom at the 4-position of the quinoline ring. These results suggest the nonparticipation of the quinoline in the binding of Cu^{2+} ion as is confirmed by the spectroscopic and computational study that will be discussed below.

Kinetics of Decomposition of Cu^{2+}−L1 Complexes. According to the species distribution diagram in Figure 3, addition of acid excess to a solution containing Cu^{2+}−**L1** complexes is expected to lead to complex decomposition with formation of $H_4\mathbf{L1}^{4+}$ and Cu^{2+}. The kinetics of decomposition of metal complexes upon addition of an acid excess has been a recurrent issue in the last decades[39−41] because the process can be easily monitored by measuring the disappearance of the absorption band of the complex, thus providing interesting information about the lability of the metal−ligand bonds and potential applications of the complexes.[42] In recent years we have also demonstrated that kinetic studies of this kind of acid-promoted decomposition, when carried out with solutions containing different $CuH_x\mathbf{L1}^{(2+x)+}$ species, can also provide in favorable cases information about molecular reorganizations associated to pH changes.[43] For this reason, we decide to study the decomposition of the Cu^{2+}−**L1** complexes and selected initially the $Cu\mathbf{L1}^{2+}$ and $Cu\mathbf{L1}(OH)^+$ species because they are the only species that can be made to exist in solution without significant amounts of any other complex species (see Figure 3). Although the data reported below correspond to experiments in the presence of 0.15 M $NaClO_4$, some experiments carried out in 0.15 M NaCl led to the same results within the error limits.

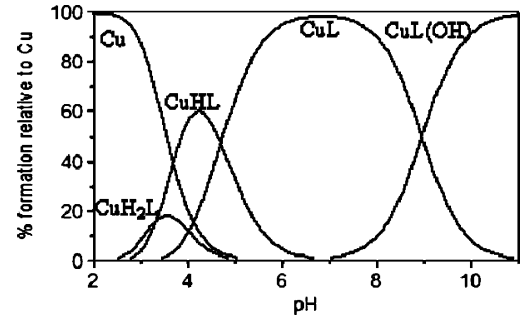

Figure 3. Species distribution curves for the Cu^{2+}−**L1** complexes in 0.15 M $NaClO_4$.

The $Cu\mathbf{L1}^{2+}$ and $Cu\mathbf{L1}(OH)^+$ species were found to decompose with the same kinetics, which indicates that the hydroxo complex is protonated upon addition of an acid excess to form $Cu\mathbf{L1}^{2+}$ within the mixing time of the stopped-flow instrument. The spectral changes recorded (Figure 4) thus correspond to the decomposition of the $Cu\mathbf{L1}^{2+}$ species, and they clearly indicate biphasic kinetics with the band centered at 890 nm disappearing faster than that at 660 nm. The biphasic character of the spectral changes was confirmed by the singular values analysis that showed clearly the existence of three colored species. These changes can be satisfactorily fitted by a kinetic model with two consecutive exponentials (eq 2) to obtain the rate constants for both steps and the spectra of the starting complex, the

(39) (a) Chen, L. H.; Chung, C. S. *Inorg. Chem.* **1989**, *28*, 1402–1405. (b) Fernández-Trujillo, M. J.; Szpoganicz, B.; Manez, M. A.; Kist, L. T.; Basallote, M. G. *Polyhedron* **1996**, *15*, 3511–3517. (c) Read, R. A.; Margerum, D. W. *Inorg. Chem.* **1981**, *20*, 3143–3149.
(40) Siddiqui, S.; Shepherd, R. E. *Inorg. Chem.* **1983**, *22*, 3726–3733.
(41) (a) Hay, R. W.; Pujari, M. P.; Bembi, R. *Transition Met. Chem.* **1986**, *11*, 261–264. (b) Chen, L. H.; Chung, C. S. *Inorg. Chem.* **1988**, *27*, 1880–1883.
(42) (a) Borthwick, T. R.; Benson, G. D.; Schugar, H. J. *Proc. Soc. Exp. Biol. Med.* **1979**, *162*, 227–228. (b) Harders, H.; Cohnen, E. *Proc. R. Soc. Med.* **1977**, *70*, 10–12. (c) Pilichowski, J. F.; Borel, M.; Meyniel, G. *Eur. J. Med. Chem.* **1984**, *19*, 425–431. (d) Sarkar, B. *Chem. Rev.* **1999**, *99*, 2535–2544. (e) Sun, X. K.; Kim, J.; Martell, A. E.; Welch, M. J.; Anderson, C. J. *Nucl. Med. Biol.* **2004**, *31*, 1051–1059.
(43) Aguilar, J.; Basallote, M. G.; Gil, L.; Hernandez, J. C.; Manez, M. A.; García-España, E.; Soriano, C.; Verdejo, B. *Dalton Trans.* **2004**, 94–103.

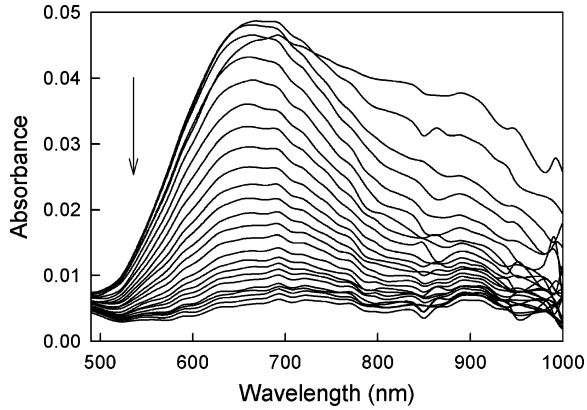

Figure 4. Typical spectral changes showing the successive disappearance of the two absorption bands during the acid-promoted decomposition of Cu**L1**$^{+2}$ species.

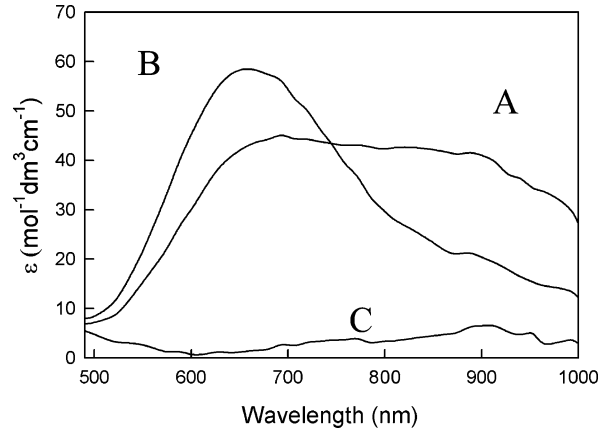

Figure 5. Spectra calculated for the starting complex (A), the reaction intermediate (B), and the reaction product (C) by fitting the spectral changes in Figure 4 to a kinetic model with two consecutive kinetic steps.

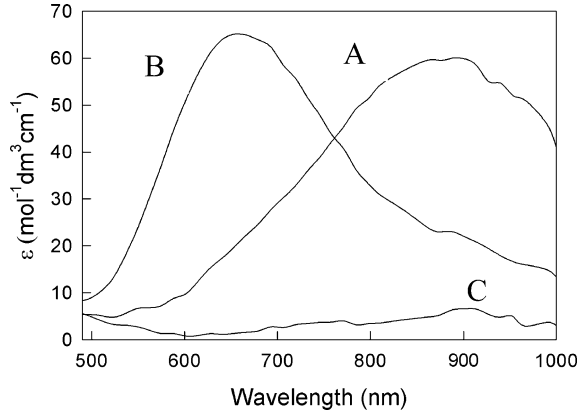

Figure 6. Spectra calculated for the A, B, and C species participating in the decomposition of Cu^{2+}−**L1** complexes according to the kinetic model defined by eq 2 but assuming that the starting solution contains an equimolar mixture of the A and B species.

reaction intermediate, and the final product shown in Figure 5. At this point it is important to note that although this kind of spectrum is commonly interpreted in the literature as corresponding to complexes with tbp geometry, the fact that both overlapping components of the absorption band disappear at different rates clearly indicates the coexistence of two geometries. As it is not possible that a mononuclear species contain two different coordination environments for the metal ion, the possibility of formation of dinuclear complexes was then considered. However, it was ruled out on the basis of the structural literature precedents[9,16a,19,20,44,45] and of the low concentrations used in the potentiometric and kinetic experiments.

$$A \rightarrow B \rightarrow C \qquad k_{1obs},\ k_{2obs} \qquad (2)$$

For these reasons, the data were analyzed with an alternative model that implies consideration of the starting solution as a mixture of two species with different geometries.

$$A \rightarrow C \qquad k_{1obs} \qquad (3)$$

$$B \rightarrow C \qquad k_{2obs} \qquad (4)$$

In this alternative model (eqs 3 and 4) there are two parallel pathways corresponding to decomposition of the two species (A and B) present in the initial reaction mixture. As the initial spectra and relative amounts of both species are unknown, the model is not well defined and some approximation is required. If the concentrations of A and B are taken to be the same and the values of the rate constants for decomposition of both species are fixed at the values derived from the model with two consecutive steps (k_{1obs} for A and k_{2obs} for B), a fit with the same quality as that of the previous one can be obtained. However, although this fit provides spectra of the starting species that clearly show absorption maxima at wavelengths typical of complexes with tbp (A) and sp (B) coordination environments, the spectrum of A has large negative molar absorptivities over a broad wavelength range, thus showing this model is inadequate. Nevertheless, another satisfactory fit of the same quality can be obtained with the kinetic model in eq 2 but considering that the starting solution contains a mixture of the two species. If the concentrations of A and B are taken to be the same, the fit provides the spectra shown in Figure 6 with the same values of the rate constants obtained for the other models. Thus, kinetic data for the acid-promoted decomposition can be also satisfactorily explained by considering the existence of an equilibrium mixture of two species with spectra typical of tbp and sp geometries. Upon addition of acid excess, complex decomposition would occur through A→ B isomerization and B decomposition.

As pointed out above, the actual values of the k_{1obs} and k_{2obs} rate constants are independent of the kinetic model used. These values are plotted in Figure 7, which clearly shows that they both show a linear dependence with the proton concentration. The fit of these data by eq 5 leads to $a = (1.2 \pm 0.6) \times 10^2\ s^{-1}$ and $b = (18 \pm 1) \times 10^2\ M^{-1}\ s^{-1}$ for the k_{1obs} data and to $b = (11 \pm 4) \times 10^2\ M^{-1}\ s^{-1}$ and a negligible value of a for the k_{2obs} data. The mechanistic information provided by these results is very limited, although according to the commonly proposed mechanism,[39] the close values of the slopes in Figure 7 would be revealing

(44) Marvaud, V.; Decroix, C.; Scuiller, A.; Guyard-Duhayon, C.; Vaissermann, J.; Gonnet, F.; Verdaguer, M. *Chem. Eur. J.* **2003**, *9*, 1677–1691.

(45) (a) Hagen, K. S.; Armstrong, W. H.; Hope, H. *Inorg. Chem.* **1988**, *27*, 967–969. (b) Zehnder, M.; Thewalt, U.; Fallab, S. *Helv. Chim. Acta* **1979**, *62*, 2099–2108.

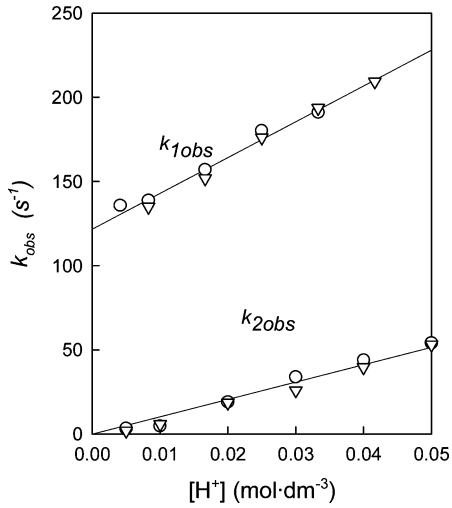

Figure 7. Plot of the dependence with the acid concentration of the observed rate constant for the acid-promoted decomposition of the Cu^{2+}−**L1** complexes in the presence of 0.15 M $NaClO_4$ at 298.1 ± 0.1 K. The circles and triangles correspond to the decomposition of $CuL1^{2+}$ and $CuL1(OH)^+$, respectively.

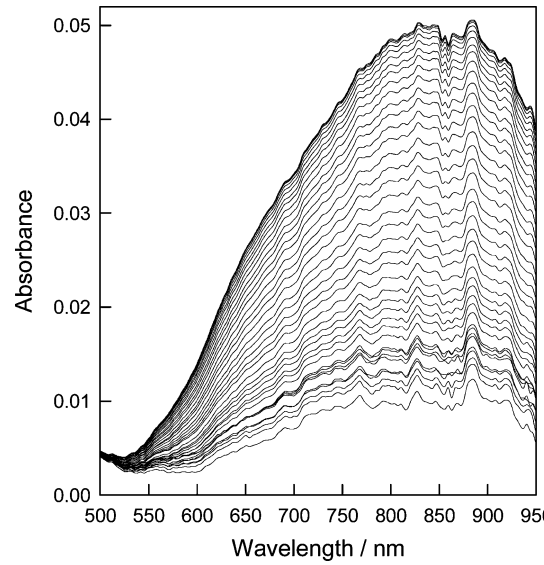

Figure 8. Typical spectral changes observed during the formation of Cu^{2+}−**L1** complexes in acidic solutions (0.15 M $NaClO_4$, pH = 4.54, 298.1 ± 0.1 K). The spectra show the appearance of a single band centered at ca. 880 nm.

that decomposition through direct acid attack occurs at similar rates, whereas the existence of a nonzero intercept in the k_{1obs} plot would be revealing that in this case there is a significant contribution to the rate of decomposition of a parallel pathway that is negligible for k_{2obs}.

$$k_{obs} = a + b[H^+] \quad (5)$$

The numerical values of the rate constants in this work are close to those previously reported for decomposition of the Cu**L2**$(H_2O)^{2+}$ complex[40] and the Cu^{2+} complex of a symmetrical binucleating cryptand with two **L2** subunits.[46] Interestingly, biphasic kinetics was observed in both of these previous studies, despite the fact that most Cu^{2+}−polyamine complexes decompose in a single kinetic step. Unfortunately, no discussion was made in those previous studies about the possibility of parallel or consecutive decomposition pathways.

Kinetics of Complex Formation in Acidic Conditions. The kinetics of formation of Cu^{2+}−**L1** complexes in acidic solutions was also studied by stopped-flow procedures by mixing Cu^{2+}(aq) and **L1** solutions, both of them prepared at the same starting pH value within the 3.6−5.9 range. No buffers were used in these kinetic experiments because it has been previously demonstrated that the highly protonated forms of this kind of macrocyclic ligand can interact with the anionic form of buffers commonly used because of their "inert" nature toward the metal ion.[47] To avoid interferences caused by the possible formation of complexes with other stoichiometries, the kinetic studies were not carried out under pseudo-first-order conditions but at Cu/**L1** ratios close to 1:1. Under these conditions, complex formation is expected to occur according to the species distribution curves in Figure 3. In agreement with this expectation, complex formation is signaled in all cases by the appearance of an absorption band centered at 880 nm (see Figure 8), but there is no evidence of development of any band at wavelengths close to 650 nm. As for the case of complex decomposition, although the data reported below correspond to experiments in the presence of 0.15 M $NaClO_4$, some experiments carried out in 0.15 M NaCl led to similar results within the error limits, thus showing that the nature of the supporting electrolyte or the interaction of the protonated forms of **L1** with Cl^- are not the responsible of any of the observed kinetic features.

These results suggest that, in acidic conditions, where formation of Cu**HL1**$^{3+}$ and Cu_2**L1**$^{4+}$ is expected to occur, there is a single tbp coordination environment around the metal center. This conclusion is further supported by the electronic spectra of equilibrium mixtures of Cu^{2+} and **L1** at different pH values, which show two overlapping bands for solutions containing either Cu**L1**$^{2+}$, Cu**L1**$(OH)^+$, or a mixture of both species, but a single band at ca. 880 nm when the solutions contain exclusively the protonated Cu**HL1**$^{3+}$ and Cu_2**L1**$^{4+}$. The appearance of this single band in the experiments of complex formation and the disappearance at different rates of the overlapping bands at 660 and 890 nm during complex decomposition provides strong support to the interpretation of the kinetic data for the decomposition process in terms of the model involving the coexistence in solution of two Cu**L1**$^{2+}$ species with different geometries.

It is interesting to note that the appearance of a single band centered at 840 nm has been observed for the Cu^{2+} complex of unsubstituted tren but a new overlapping band at 660 nm gradually appears on increasing pH.[48] Although the authors interpreted these results in terms of structural distortion toward an sp geometry when the hydroxo complex is formed, the results in the present Article suggest that those results

(46) Basallote, M. G.; Duran, J.; Fernández-Trujillo, M. J.; Manez, M. A. *J. Chem. Soc., Dalton Trans.* **1999**, 3817–3823.
(47) Basallote, M. G.; Duran, J.; Fernández-Trujillo, M. J.; Manez, M. A.; Szpoganicz, B. *J. Chem. Soc., Dalton Trans.* **1999**, *7*, 1093–1100.
(48) Mao, Z. W.; Liehr, G.; van Eldik, R. *J. Chem. Soc., Dalton Trans.* **2001**, 1593–1600.

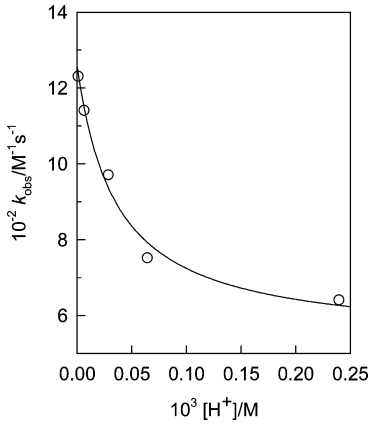

Figure 9. Plot of the dependence on the acid concentration of the observed rate constant for the formation of the CuL complex at 298.1 ± 0.1 K in the presence of 0.15 M $NaClO_4$.

Table 3. pH Dependence of the k_{obs} Values Obtained for the Formation of Cu^{2+}−**L1** Complexes in Solutions Containing a 1:1 (Cu/L) Molar Ratio (298.1 K, 0.15 M $NaClO_4$)

pH	$10^{-2}\ k_{obs}$ ($M^{-1}\ s^{-1}$)
3.62	6.4 ± 0.2
4.19	7.51 ± 0.08
4.54	9.7 ± 0.1
5.18	11.4 ± 0.1
5.90	12.3 ± 0.1

can be also interpreted considering that the structure of $Cu(tren)(H_2O)^{2+}$ is tbp but that $Cu(tren)(OH)^+$ probably exists as a mixture of two isomers with tbp and sp geometries. In contrast, the related $Cu(tren)NH_3^{2+}$ complex shows a band at 880 nm with a shoulder at 660 nm.[18] Further work is in progress to gain insight into the details of these spectral changes and the behavior of the two bands in experiments of complex formation and decomposition with unsubstituted tren and other tren-based ligands. In any case, the present results and the frequent appearance of overlapping bands in the electronic spectra of Cu^{2+} complexes with this kind of ligand suggests that the existence of equilibrium mixtures of isomers with different coordination environments can be more common than usually assumed.

With regards to the analysis of the kinetic data, the experimental data of the type shown in Figure 8 could be always well fitted according to a monophasic process of first order with respect to each reactant, Cu^{2+} and L (eq 6). The values derived for k_{obs} at different starting pH values are included in Table 3, which shows a clear increase in the rate constant when the pH is increased. At the pH range covered in the kinetic studies Cu^{2+} exists exclusively as the aqua complex so that the pH dependence must be ascribed exclusively to the different reactivity of the H_x**L1**$^{x+}$ species. To estimate them, the values of k_{obs} were represented against $[H^+]$ (Figure 9), and the resulting plot suggests a dependence of the form given by eq 7. Actually a satisfactory fit could be obtained using this equation and the values $a = (1.26 \pm 0.01) \times 10^3\ M^{-1}\ s^{-1}$, $b = (5.3 \pm 0.6) \times 10^2\ M^{-1}\ s^{-1}$ and $c = (4.4 \pm 0.8) \times 10^4\ M^{-1}$.

$$Cu + L \rightarrow CuL; \quad k_{obs} \tag{6}$$

With the help of the species distribution curves for the different protonated ligand species as a function of pH, these results can be interpreted by considering that complex formation occurs according to the mechanistic scheme in eqs 8−10, which leads to a rate law of the same form than the experimental one with the equivalencies $a = k_{Cu-H3L1}$, $b = k_{Cu-H4L}$, and $c = K_{H4L}$. Under the experimental conditions used, the ligand exists as a mixture of H_3**L1**$^{3+}$ and H_4**L1**$^{4+}$ and both of them contribute to the net rate of complex formation, but as expected from electrostatic considerations, the less protonated form reacts faster. Although the value of the equilibrium constant derived from the kinetic measurements ($\log K_{H4L} = 4.67$) is significantly larger than the value derived from the potentiometric measurements ($\log K_{H4L} = 3.43$), similar differences have been previously observed in this kind of study[49] and can be easily rationalized by the accumulation of errors and the absence of buffering agent in the kinetic experiments.

$$k = \frac{a + bc[H^+]}{1 + c[H^+]} \tag{7}$$

$$H_3L^{3+} + H^+ \rightleftarrows H_4L^{4+}; \quad K_{H4L} \tag{8}$$

$$Cu^{2+} + H_3L^{3+} \rightarrow CuL^{2+} + 3H^+; \quad k_{Cu-H3L} \tag{9}$$

$$Cu^{2+} + H_4L^{4+} \rightarrow CuL^{2+} + 4H^+; \quad k_{Cu-H4L} \tag{10}$$

During the course of this work we were aware of the appearance of an Article[50] facing the problem of avoiding buffer effects in the kinetics of complex formation by means of using a program (Pro-KII) that allows one to take into account the pH dependence and the changes in the proton concentration during the process of complex formation by making a simultaneous fit of the experimental data obtained at different pH values. We reanalyzed the kinetic data with this program and obtained results quite similar to those above: $k_{Cu-H3L} = (1.20 \pm 0.01) \times 10^3\ M^{-1}\ s^{-1}$ and $k_{Cu-H4L} = (8.7 \pm 0.2) \times 10^2\ M^{-1}\ s^{-1}$ with K_{H4L} fixed at the value (3.43) derived from the potentiometric measurements. These values compare well with those reported[51] for complexation of Cu^{2+} with tren ($k_{Cu-H3L} = 1 \times 10^2\ M^{-1}\ s^{-1}$ and $k_{Cu-H2L} = 3.8 \times 10^6\ M^{-1}\ s^{-1}$), the differences being easily understood in terms of the different nature and protonation constants of the ligands.

DFT Calculations. The experimental data in previous sections indicate that the Cu**L1**$^{2+}$ complex exists in solution as a mixture of two species with different geometries. According to the position of the absorption maximum, one of the species has a tbp structure and the other one is sp. In the absence of crystallographic structures and considering the existence of mixtures of species in solution, DFT studies were carried out to obtain some information about the nature of the species and the processes that occur in solution. The calculations were carried out by optimizing the geometries both in the gas phase and in solution (CPCM model) to obtain

(49) Verdejo, B.; Ferrer, A.; Blasco, S.; Castillo, C. E.; Gonzalez, J.; Latorre, J.; Manez, M. A.; Basallote, M. G.; Soriano, C.; Garcia-Espana, E. *Inorg. Chem.* **2007**, *46*, 5707–5719.
(50) McCann, N.; Lawrance, G. A.; Neuhold, Y. M.; Maeder, M. *Inorg. Chem.* **2007**, *46*, 4002–4009.
(51) Roche, T. S.; Wilkins, R. G. *J. Am. Chem. Soc.* **1974**, *96*, 5082–5086.

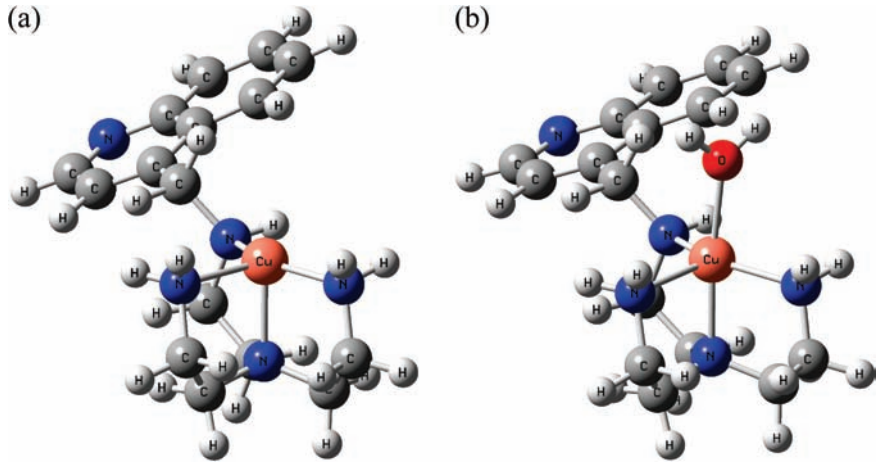

Figure 10. Optimized geometries for the Cu**L1**$^{2+}$ complex in the absence of any additional ligand (a) and with one coordinated water molecule (b). The geometry in (b) is that named as tbp1 in the text.

a better approximation to the experimental conditions. However, the energies and geometries derived must be taken with care not only because of the limitations implicit in the calculations but also because additional factors as hydrogen bonding with solvent molecules were not included in the model. Nevertheless, despite these limitations the results were very revealing.

The starting point for the calculations was the consideration that all five nitrogen donors in **L1** could coordinate simultaneously to the Cu^{2+} center. However, all attempts to obtain stable structures of this kind were unsuccessful, the computations clearly showing that the nitrogen in the quinoline ring cannot coordinate to a Cu^{2+} center that is already bonded to the four nitrogens in the tren unit. Optimizations lead to structures such as that shown in Figure 10a, in which the quinolinic nitrogen is far away from the fifth coordination site. Attempts to coordinate the quinoline group to a Cu^{2+} center in which there is no Cu−N bond with the NH group of the arm supporting the quinoline substituent were also unsuccessful as they resulted in geometries of high energy and containing unreasonable Cu−C bonds. From these results, it appears reasonable to assume that the experimental absorption band centered at 890 nm corresponds to a complex with a tbp structure similar to that observed for unsubstituted tren, in which the fifth coordination site is occupied by a water molecule. Cu(tren)$(H_2O)^{2+}$ shows a band at 880 nm.[6] For the case of the **L1** ligand, optimizations lead to the structure tbp1 (Figure 10b), with $\tau = 0.51$ (gas phase) or 0.45 (solution), which indicates a distorted structure midway between the tbp and sp extremes. Although the τ values clearly indicate strongly distorted tbp geometry for species tbp1, this kind of distortion is quite usual in pentacoordinate Cu^{2+} complexes. Thus, although some Cu(tren)X^{z+} complexes show τ values higher than 0.8,[4,7−9,52] values as low as 0.42 and 0.43 are obtained when X is 4,5-diazafluorene-9-hydrazine or 4,5-diazafluoren-9-one.[53] It is important to note that despite the significant deviation from the ideal geometry, the position of the absorption maximum in the electronic spectra of these complexes still falls within the range typical of tbp geometry.

Table 4. Summary of Relative Energies, τ, and λ_{max} (nm) values for the Different Gas-Phase and Solution Optimized Geometries Obtained for the Pentacoordinate Cu^{2+} Complexes with the **L1** and **L2** Ligands[a]

		relative energy (kcal mol^{-1})		τ		λ_{max} (nm)[b]	
species	denticity	gas	solution	gas	solution	gas	solution
tbp1	tetradentate	0.0	0.0	0.51	0.45	776.34	672.89
sp1	tridentate	5.0	3.2	0.28	0.18	711.26	566.46
tbp2	tridentate	14.8	8.8	0.82	0.63	1034.12	769.77
sp2	tridentate	12.0	10.7	0.00	0.06	503.56	588.05
tbp1b	tetradentate	4.7	6.0	0.51	0.49	601.69	574.24
tbp1c	tetradentate	6.9	9.3	0.58	0.61	747.44	726.86
sp1b	tridentate	10.1	7.3	0.13	0.09	791.97	779.27
tren-tbp	tetradentate	0.0	0.0	0.59	0.58	805.34	758.72
tren-sp1	tridentate	6.9	4.3	0.23	0.14	577.17	564.47
tren-sp2	tridentate	10.1	8.2	0.13	0.30	538.36	696.75

[a] The relative gas energy values correspond to CPCM single-point calculations on the previously gas-phase optimized structures. [b] These values correspond to the λ (nm) of the most intense transition of each calculated spectra using the CPCM/TD-DFT approach. All the calculated excited-state energies and oscillator strengths are included in the Supporting Information.

As the experimental results in the present work indicate the coexistence of two species with different geometries, efforts were made to optimize geometries different from tbp1. However, all attempts to obtain a stable species with a coordination environment formed by four nitrogens of **L1** and one water molecule were unsuccessful because calculations lead in all cases to tbp1 or closely related species of higher energy with very similar coordination environments and that only differ in the conformation of the pendant arm containing the quinoline ring (species tbp1b and tbp1c, see energies in Table 4 and geometries in the Supporting Information). Attempts to optimize species with one additional coordinated water and a distorted octahedral geometry were also unsuccessful, as the calculations lead to the

(52) Duggan, D. M.; Hendrickson, D. N. *Inorg. Chem.* **1974**, *13*, 1911–1916.

(53) (a) Lu, Z. L.; Duan, C. Y.; Tian, Y. P.; You, X. Z.; Fun, H. K.; Yip, B. C.; Hovestreydt, E. *Polyhedron* **1997**, *16*, 187–194. (b) Lu, Z. L.; Duan, C. Y.; Tian, Y. P.; You, X. Z.; Huang, X. Y. *Inorg. Chem.* **1996**, *35*, 2253–2258.

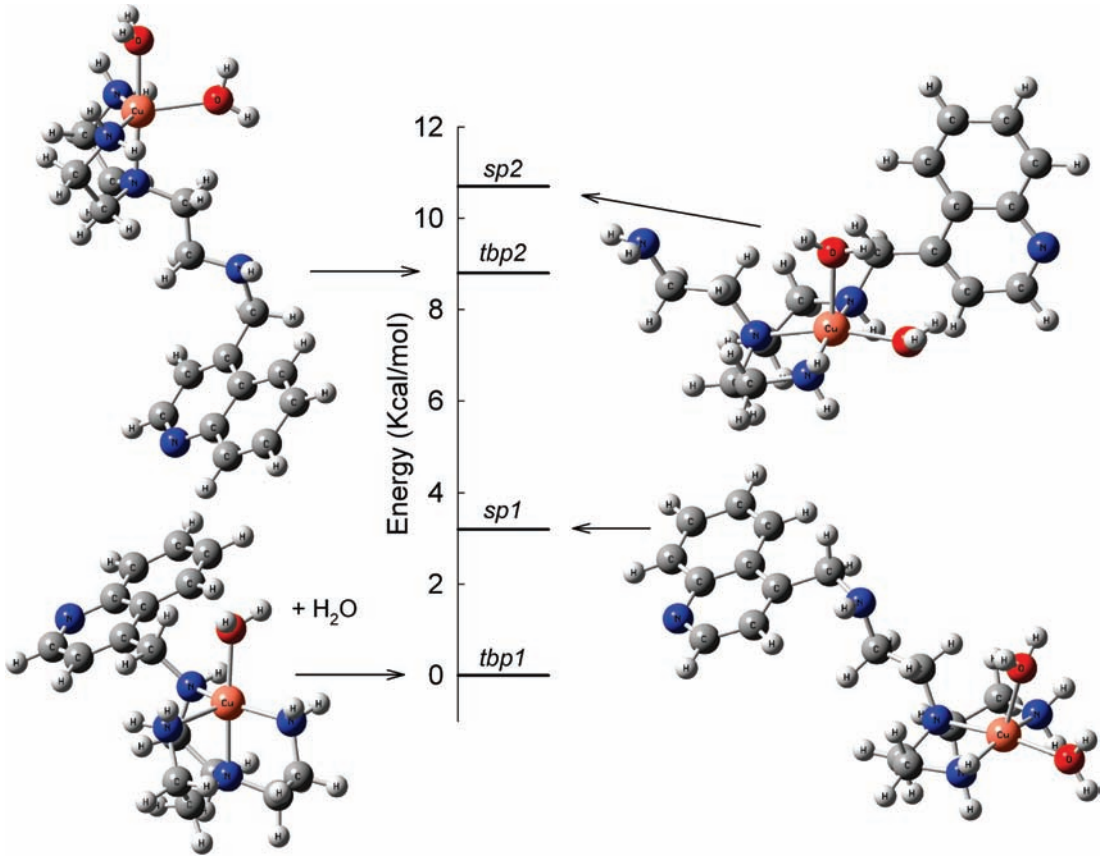

Figure 11. Geometries and relative energies (CPCM-optimized model) for the Cu^{2+}−**L1** complexes discussed in the text.

tbp1 structure with the second water forming a hydrogen bond with the first one.

As the whole set of calculations indicate that **L1** cannot act as pentadentate and calculations with **L1** acting as a tetradentate ligand only provided a single stable structure for the Cu**L1**$^{2+}$ complex, those results cannot explain the experimental observation of a mixture of two species in solution. For this reason, calculations were also made with two coordinated water molecules and the ligand acting as tridentate. Interestingly, the most stable structure obtained with this coordination is square pyramidal (sp1 in Figure 11, see τ values in Table 4), and the energy associated to the hydrolysis of the Cu−N bond in tbp1 to form sp1 is small in aqueous solution (see also the energy values in Table 4) so that a mixture of both species can be reasonably expected to exist in solution. Whereas in the case of tetradentate **L1** all optimizations lead to a single geometry (tbp1), calculations with the ligand acting as tridentate also allow the optimization of a tbp structure (tbp2), although the energy values in Table 4 show that it is significantly higher in energy than its geometric isomer sp1, which indicates that the amount of tbp2 formed in solution must be expected to be very small compared to sp1 and tbp1. On the other hand, as sp1 results from the hydrolysis of the Cu−N bond with the amine group supporting the appended arm, calculations were also made to obtain a similar structure where the hydrolyzed bond is one with a terminal NH_2 group. These calculations lead to the almost ideal square pyramidal sp2 structure (Figure 11, Table 4), which is higher in energy than sp1, thus showing that hydrolysis is significantly more favored for the Cu−N bond with the substituted terminal amine group of the tren subunit. Attempts to obtain the tbp analogue of sp2 always converged to the latter structure. As a summary, DFT calculations provide a reasonable explanation to the experimental observation of Cu**L1**$^{2+}$ existing as a mixture of two species with different coordination geometries. However, the formation of such a mixture is the result of the hydrolysis process shown in Figure 12, which is accompanied of a change from tbp to sp coordination. The small energy change associated to this process indicates that both species will be formed in comparable and detectable amounts, in agreement with the spectral and kinetic experimental data.

Although the results of the calculations described above reveal a preferential hydrolysis of the Cu−N bond with the substituted amine group supporting the appended arm, the relevance of the hydrolytic process in Figure 12 in the chemistry of Cu^{2+} complexes with unsubstituted tren was also examined. As occurs with Cu**L1**$^{2+}$, all optimizations of the [Cu**L2**$(H_2O)]^{2+}$ complex converged in a single species with distorted tbp structure (tren-tbp, see τ values in Table 4 and the geometry in the Supporting Information). However, hydrolysis of the Cu−N bond with one of the terminal NH_2 groups leads to two isomeric [Cu**L2**$(H_2O)_2]^{2+}$ complexes containing tridentate tren (tren-sp1 and tren-sp2) and with geometries typical of sp complexes. The energy values in Table 4 show that tren-sp2 is significantly higher in energy than tren-tbp so that large amounts of these species are not

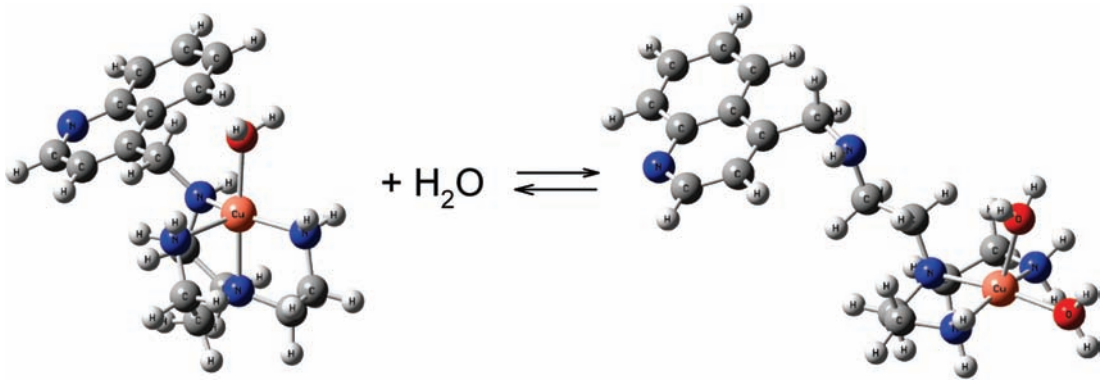

Figure 12. Proposed hydrolysis equilibrium of the Cu**L1**$^{2+}$ complex showing the geometric change in the coordination environment from trigonal bipyramidal when the ligand acts as tetradentate to square planar when the ligand is tridentate.

expected to be formed in solution. However, the energy difference between the tren-sp1 and tren-tbp structures is not so large and the possibility of formation of the sp species cannot be completely ruled out. A more detailed study of the tren complexes is being currently carried out, and the results will be reported in the future. In any case, it appears that the relevance of the hydrolytic process in Figure 12 decreases somewhat in unsubstituted tren so that the DFT calculations reported in the present work indicate that the introduction of a substituent at one of the terminal NH_2 groups makes more energetically accessible a hydrolysis process that leads to formation of a mixture of species with different geometries, spectra, and kinetic properties.

To obtain more information about the occurrence of the geometric changes proposed in previous paragraphs, the electronic spectra of all the species in Table 4 were calculated applying the TD-DFT approach.[35] Excitation energies and oscillator strengths are given in the Supporting Information together with the Cartesian coordinates and the geometries of each individual species. In general, the calculated spectra show the appearance of a single absorption band centered at wavelengths that span over a wide interval (ca. 500−1000 nm) that includes the values usually observed in the experimental spectra of these kinds of copper complexes. Inspection of the data in Table 4 indicates that the position of the absorption maximum can be significantly affected by the ligand conformation so that shifts in the absorption maximum of up to 175 nm are obtained for small changes in the coordination environment of the metal center (for example, the tbp1 and tbp1b species). As in real solutions it is expected that each species exists as a mixture of rapidly interconverting conformers, the correlation between experimental and calculated spectra must be taken with caution. Despite these limitations, the position of the band appears to be mainly determined by the τ value, the effects of changes in the denticity of the ligand and of the introduction of a substituent at a terminal NH_2 group of tren being much smaller. Although changes in the τ values as large as 0.2 are observed when the geometry optimizations are carried out in the gas phase or in solution, and this causes shifts of up to ca. 280 nm in λ_{max}, there is still a quite good correlation between all the λ_{max} and τ values in Table 4. It is important to note that in real systems the values of λ_{max} and τ will be affected not only by the approximations involved in this

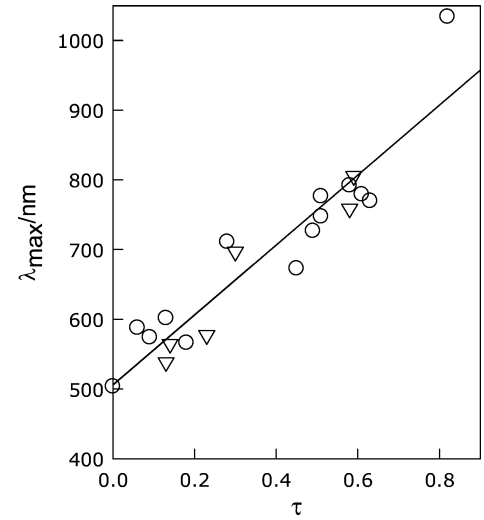

Figure 13. Plot showing the correlation between the λ_{max} (nm) and τ values for the different optimized geometries obtained for the Cu complexes with the **L1** (○) and **L2** (▽) ligands.

correlation but also by factors not considered in the present calculations, such as hydrogen bonding with water solvent molecules and crystal packing forces in the case of solid-state structures. The $\lambda_{max}-\tau$ correlation is illustrated in Figure 13, and it can be represented by eq 11 ($r^2 = 0.878$), which can be used to estimate the actual geometry *in solution* of these pentacoordinate Cu^{2+}−polyamine complexes from their experimental electronic spectra. Thus, although the values derived can be only considered approximate, the appearance of the two bands at 660 and 890 nm in the spectra registered in the kinetic experiments would be indicating the coexistence of two species with τ values close to 0.31 and 0.76, respectively. Although this correlation does not discriminate between different possibilities arising from changes in the denticity of the ligand, the results of the DFT calculations described above strongly support that both species appear as a consequence of the operation of the equilibrium represented in Figure 12.

$$\lambda_{max} = 506 + 502\tau \qquad (11)$$

Conclusion

In this work detailed equilibrium and kinetic studies are presented relative to the formation and decomposition of

Cu^{2+} complexes with a monosubstituted tren ligand. The analysis of the kinetic results indicates that the Cu**L1**$^{2+}$ complex exists in solution as a mixture of two species with different geometries, tbp and sp. Both geometries would be the responsible of the two components observed in the electronic spectrum. On the other hand, DFT studies suggest that the appearance of both geometries is not caused by the existence of two isomeric forms of the same complex but has its origin in the existence of an equilibrium of hydrolysis of the Cu−N bond with the amino group supporting the 4-quinolylmethyl group, in such a way that Cu**L1**$^{2+}$ would be actually a mixture of tbp [Cu**L1**$(H_2O)]^{2+}$ and sp [Cu**L1**$(H_2O)_2]^{2+}$. As these species have the same Cu/**L**/H ratio, they are not distinguishable in the analysis of the potentiometric results, which only provides an equilibrium constant that measures the stabilization associated to the formation of the whole set of species with the same stoichiometry. In contrast, kinetic experiments of acid-promoted decomposition clearly reveal a different behavior for the absorption bands associated to both species, a result further supported by the kinetics of complex formation. As there are many literature reports of Cu^{2+}−polyamine complexes with spectra similar to that of Cu**L1**$^{2+}$, this kind of equilibrium can be quite common in the chemistry of this kind of compound, and so this possibility must be explored in the future. From this point of view, the correlation found between the λ_{max} and τ values can be used to estimate the structure *in solution* from the position of the absorption maximum in the experimental spectra. Future studies should also provide information about the factors leading to stabilization of the different forms and the effects that this kind of equilibrium has in the reactivity of these complexes.

Acknowledgment. We acknowledge the Ministerio de Ciencia y Tecnología and the FEDER program (Grants CTQ2006-14909-C02-01 and CTQ2006-15672-CO5-01) as well as the Junta de Andalucía (FQM-137) and Generalitat Valenciana (GV06/258) for financial support. Computer facilities by the Centro de Supercomputación de la Universidad de Cádiz are also acknowledged. Predoctoral Grants are also acknowledged to Universidad de Cádiz (A.F. and C.E.C.) and Ministerio de Ciencia y Tecnología (A.G.A.). J.M.Ll. thanks MCYT of Spain for a Ramón y Cajal contract.

Supporting Information Available: Tables with the equilibrium constant for the interaction of Cl^- with the protonated forms of the ligand and with absolute energies for all the calculated species discussed in the work, a figure with the relative energies and geometries for the Cu^{2+}−tren species, and collection of Cartesian coordinates, geometries, and results of the TD-DFT calculations for all of the species. This material is available free of charge via the Internet at http://pubs.acs.org.

IC8013078